

Protein-based ultrafast photonic switching

László Fábíán,¹ Zsuzsanna Heiner,¹ Mark Mero,² Miklós Kiss,³
Elmar K. Wolff,⁴ Pál Ormos,¹ Károly Osvay,³ and András Dér^{1,*}

¹*Institute of Biophysics, Biological Research Centre of the Hungarian Academy of Sciences, P.O. Box 521, 6701 Szeged, Hungary*

²*HAS Research Group of Laser Physics, P.O. Box 406, 6701 Szeged, Hungary*

³*Department of Optics and Quantum Electronics, University of Szeged, P.O. Box 406, 6701 Szeged, Hungary*

⁴*Institute for Applied Biotechnology and System Analysis at the University of Witten/Herdecke, Herrhausenstrasse 44, 58455 Witten, Germany*

**derandra@brc.hu*

Abstract: Several inorganic and organic materials have been suggested for utilization as nonlinear optical material performing light-controlled active functions in integrated optical circuits, however, none of them is considered to be the optimal solution. Here we present the first demonstration of a subpicosecond photonic switch by an alternative approach, where the active role is performed by a material of biological origin: the chromoprotein bacteriorhodopsin, via its ultrafast BR- \rightarrow K and BR- \rightarrow I transitions. The results may serve as a basis for the future realization of protein-based integrated optical devices that can eventually lead to a conceptual revolution in the development of telecommunications technologies.

©2011 Optical Society of America

OCIS Codes: (060.1155) All-optical networks; (130.4815) Optical switching devices; (130.3120) Integrated optics devices; (320.7120) Ultrafast phenomena; (320.7085) Ultrafast information processing; (160.1435) Biomaterials.

References and links

1. S. A. Haque and J. Nelson, "Toward organic all-optical switching," *Science* **327**(5972), 1466–1467 (2010).
2. J. M. Hales, J. Matichak, S. Barlow, S. Ohira, K. Yesudas, J.-L. Bredas, J. W. Perry, and R. R. Marder, "Design of polymethine dyes with large third-order optical nonlinearities and loss figures of merit," *Science* **327**(5972), 1485–1488 (2010).
3. X. Hu, P. Jiang, C. Ding, H. Yang, and Q. Gong, "Picosecond and low-power all-optical switching based on an organic photonic bandgap microcavity," *Nat. Photonics* **2**(3), 185–189 (2008).
4. W. Stoekenius, R. H. Lozier, and R. A. Bogomolni, "Bacteriorhodopsin and the purple membrane of halobacteria," *Biochim. Biophys. Acta* **505**, 215–278 (1979).
5. N. Vsevolodov, *Biomolecular electronics* (Birkhauser, Boston, 1998).
6. E. Korchemskaya, N. Burykin, S. Bugaychuk, O. Maksymova, T. Ebrey, and S. P. Balashov, "Dynamic holography in bacteriorhodopsin/gelatin films: Effects of light-dark adaptation at different humidity," *Photochem. Photobiol.* **83**(2), 403–408 (2007).
7. J. A. Stuart, D. L. Marcy, and R. R. Birge, "Photonic and optoelectronic application of bacteriorhodopsin," in *Bioelectronic Applications of Photochromic Pigments*, A. Dér, and L. Keszthelyi, eds. (2001), pp. 15–29.
8. D. Zeisel and N. Hampp, "Spectral relationship of light-induced refractive index and absorption changes in bacteriorhodopsin films containing wildtype BR and the variant BR-D96N," *J. Phys. Chem.* **96**(19), 7788–7792 (1992).
9. K. J. Wise, N. B. Gillespie, J. A. Stuart, M. P. Krebs, and R. R. Birge, "Optimization of bacteriorhodopsin for bioelectronic devices," *Trends Biotechnol.* **20**(9), 387–394 (2002).
10. S. P. Balashov, "Photoreactions of the photointermediates of bacteriorhodopsin," *Isr. J. Chem.* **35**, 415–428 (1995).
11. P. Ormos, Z. Dancsházy, and L. Keszthelyi, "Electric response of a back photoreaction in the bacteriorhodopsin photocycle," *Biophys. J.* **31**(2), 207–213 (1980).
12. A. Colonna, G. I. Groma, and M. H. Vos, "Retinal isomerization dynamics in dry bacteriorhodopsin films," *Chem. Phys. Lett.* **415**(1-3), 69–73 (2005).
13. G. Váró and L. Keszthelyi, "Photoelectric signals from dried oriented purple membranes of *Halobacterium halobium*," *Biophys. J.* **43**(1), 47–51 (1983).
14. L. Fábíán, E. K. Wolff, L. Oroszi, P. Ormos, and A. Dér, "Fast integrated optical switching by the protein bacteriorhodopsin," *Appl. Phys. Lett.* **97**(2), 023305 (2010).

15. P. Ormos, L. Fábrián, L. Oroszi, E. K. Wolff, J. J. Ramsden, and A. Dér, "Protein-based integrated optical switching and modulation," *Appl. Phys. Lett.* **80**(21), 4060–4062 (2002).
16. A. Dér, S. Valkai, L. Fábrián, P. Ormos, J. J. Ramsden, and E. K. Wolff, "Integrated optical switching based on the protein bacteriorhodopsin," *Photochem. Photobiol.* **83**(2), 393–396 (2007).
17. S. Roy, M. Prasad, J. Topolancik, and F. Vollmer, "All-optical switching with bacteriorhodopsin protein coated microcavities and its application to low power computing circuits," *J. Appl. Phys.* **107**(5), 053115 (2010).
18. J. Topolancik and F. Vollmer, "All-optical switching in the near infrared with bacteriorhodopsin-coated microcavities," *Appl. Phys. Lett.* **89**(18), 184103 (2006).
19. E. K. Wolff and A. Dér, "All-optical logic," *Nanotechnol. Percept.* **6**, 51–56 (2010).
20. M. Mero, A. Sipos, G. Kurdi, and K. Osvay, "Generation of energetic femtosecond green pulses based on an OPCPA-SFG scheme," *Opt. Express* **19**(10), 9646–9655 (2011).
21. K. Tiefenthaler and W. Lukosz, "Sensitivity of grating couplers as integrated optical chemical sensors," *J. Opt. Soc. Am. B* **6**(2), 209–220 (1989).
22. J. Vörös, J. J. Ramsden, G. Csúcs, I. Szendrő, S. M. De Paul, M. Textor, and N. D. Spencer, "Optical grating coupler biosensors," *Biomaterials* **23**(17), 3699–3710 (2002).
23. R. A. Mathies, C. H. Brito Cruz, W. T. Pollard, and C. V. Shank, "Direct observation of the femtosecond excited-state cis-trans isomerization in bacteriorhodopsin," *Science* **240**(4853), 777–779 (1988).
24. S. Ruhman, B. X. Hou, N. Friedman, M. Ottolenghi, and M. Sheves, "Following evolution of bacteriorhodopsin in its reactive excited state via stimulated emission pumping," *J. Am. Chem. Soc.* **124**(30), 8854–8858 (2002).
25. S. Sharkov, A. Pakulev, S. Chekalin, and Y. Matveetz, "Primary events in bacteriorhodopsin probed by subpicosecond spectroscopy," *Biochim. Biophys. Acta* **808**(1), 94–102 (1985).
26. A. Aharoni, B. Hou, N. Friedman, M. Ottolenghi, I. Rouso, S. Ruhman, M. Sheves, T. Ye, and Q. Zhong, "Non-isomerizable artificial pigments: Implications for the primary light-induced events in bacteriorhodopsin," *Biochemistry (Mosc.)* **66**(11), 1210–1219 (2001).
27. A. Biesso, W. Qian, and M. El-Sayed, "Gold nanoparticle plasmonic field effect on the primary step of the other photosynthetic system in Nature, bacteriorhodopsin," *J. Am. Chem. Soc.* **130**(11), 3258–3259 (2008).
28. J. Dobler, W. Zinth, W. Kaiser, and D. Oesterhelt, "Excited-state reaction dynamics of bacteriorhodopsin studied by femtosecond spectroscopy," *Chem. Phys. Lett.* **144**(2), 215–220 (1988).
29. D. W. McCamant, P. Kukura, and R. A. Mathies, "Femtosecond stimulated Raman study of excited-state evolution in bacteriorhodopsin," *J. Phys. Chem. B* **109**(20), 10449–10457 (2005).
30. M. L. Applebury, K. S. Peters, and P. M. Rentzepis, "Primary intermediates in the photochemical cycle of bacteriorhodopsin," *Biophys. J.* **23**(3), 375–382 (1978).

1. Introduction

The continuous growth of internet traffic is expected to last for the foreseeable future. The concept of Tbit/s telecommunication represents the expectations of a serious improvement both in capacity and speed of data trafficking. All-optical (photonic) data processing is generally considered to be the most promising approach to achieve these goals. Contrary to the electronic conductors and transistors, their optical counterparts, miniature light guides and optical switches, respectively, serve as passive and active elements to process (optically coded) information. To this end, the basic problem is to find proper nonlinear optical materials that are able to actively control optical circuits. Several materials have been considered for this special application requiring high speed and sensitivity, however, so far none of them is regarded as the optimal solution.

According to the most recent view, the more versatile and cost-effective organic materials represent a promising alternative of the currently used inorganic semiconductor materials [1]. Specifically designed organic, π -conjugated molecular materials have attracted so far the most attention [2,3]. They show a high (third-order) optical polarizability, without two-photon absorption losses. These dye molecular structures, however, should be further optimized, embedded and tested in solid films before they can be applied in high-performance all-optical devices. Hence, in view of the urgency of the technical requirements, it seems to be desirable to explore other approaches, too.

Nature readily provides us with π -conjugated materials optimized for sensing light during myriads of years of evolution [4]. Although biological materials in general are disregarded in technical applications because of their fragile nature, there are some proteins that are extraordinarily robust, so their biological origin does not represent a practical disadvantage in any respect, on the contrary, they offer special advantages which can be exploited in bioelectronic applications [5].

Among biological molecules under consideration for technical use, the chromoprotein bacteriorhodopsin (bR) has generated the most interest due to its striking robustness and other favourable physical properties [6–8]. Isolated from the cell membrane of the microorganism *Halobacterium salinarum*, bR is the simplest ion pump, and one of the best-characterized membrane proteins [4]. It has a π -conjugated chromophore, the retinal molecule, as a light-sensing prosthetic group that is stabilized by polar (aromatic) residues of the protein. The optical properties (spectra and kinetics) of bR are fine-tuned by point charges on amino acid side chains adjacent to the retinal molecule, and can be easily modified by genetic engineering techniques (site-directed mutagenesis), or by specific physical and chemical treatment of the chromoprotein [9].

Upon illumination, bR transports protons across the membrane, while undergoing a cyclic series of reactions with quasi-stable intermediate states, all with characteristic absorption spectra: $\text{BR}_{570} \rightarrow \text{I}_{460} \rightarrow \text{J}_{625} \rightarrow \text{K}_{610} \rightarrow \text{L}_{540} \rightarrow \text{M}_{410} \rightarrow \text{N}_{550} \rightarrow \text{O}_{630} \rightarrow \text{BR}_{570}$. The letters denote the ground and intermediate states (“BR” and “I” to “O”, respectively), and the subscripts refer to the wavelengths in nm of their absorption maxima. All intermediates are also light sensitive [10,11], i.e., upon a second excitation they rapidly return to the ground state (BR). Hence, bR is often referred to as an ‘optically programmable’ material [7]. Thin films of optical quality prepared from bR are used in most of the bioelectronic applications, like holography. In these dried bR samples, the photocycle lacks all the intermediates after M, that directly decays back to BR. The transition rates span from sub-picoseconds ($\text{BR} \rightarrow \text{I} \rightarrow \text{J} \rightarrow \text{K}$) through microseconds ($\text{K} \rightarrow \text{L} \rightarrow \text{M}$) to hundreds of milliseconds ($\text{M} \rightarrow \text{BR}$) [12,13]. The photocycle reactions are accompanied by change of absorption, hence the refractive index also changes corresponding to the Kramers-Kronig relations [8,14].

The first experiments concerning the integrated optical application of bR proved that under continuous illumination of the ground-state bR, the refractive index of a dried bR film at 630 nm changes while the M state develops [15]. Consequently, if a probe laser light at a wavelength outside of the excitation range of bR is coupled into an integrated optical device (e.g., a Mach-Zehnder interferometer) covered by an adlayer prepared of bR, the intensity of the output can be modulated by exciting the sample. On these grounds, we demonstrated high-quality all-optical switching based on the M intermediate [16]. Optical switching and logical operation based on the $\text{BR} \rightarrow \text{M}$ transition was shown later by other integrated optical structures, as well [17–19]. The speed of switching based on the $\text{BR} \rightarrow \text{M}$ reaction is undoubtedly trailing the state-of-the-art electronic-only devices. However, most recent kinetic experiments based on the $\text{BR} \rightarrow \text{K}$ transition have demonstrated an optical switching in the 10 nanosecond range [14]. These results raised hope to the feasibility of an ultrafast photonic switch utilizing the picosecond transition time of the $\text{BR} \rightarrow \text{K}$ photoreaction that would represent a breakthrough in biophotonic switching. In the following, we experimentally demonstrate an optical switch based on the K intermediate allowing a >100 GHz communication speed. Moreover, we present evidences for an even faster, subpicosecond switching event related to the $\text{BR} \rightarrow \text{I}$ transition, which makes possible to go beyond the magic limit of 1Tbit/s data traffic.

2. Experimental setup

In order to reveal ultrafast integrated optical switching based on the nonlinear optical properties of bR, pump-probe experiments were performed with the use of picosecond and femtosecond light pulses (Fig. 1(a)). The concept of the measurement was the following: A short pump pulse at a wavelength in the absorption band of bR (530 nm) initiated the photocycle of the protein. The induced change of refractive index was then probed by a subsequent laser pulse at a central wavelength around 790 nm, which lies outside the absorption bands of all intermediates (this way the photocycle is not affected by the probe

pulse). The probed transition was then characterized by changing the time delay between the pump and probe pulses, as well as their duration.

In all of the measurements light pulses of a TW-class laser system was used, which provided us with two synchronized pulses centered at 530 nm and 790 nm wavelengths, respectively. The broadband pulses of 530 nm (pulse energy 80 μ J) were generated from the more intense part of the fundamental beam with the unique combination of non-collinear optical parametric chirped pulse amplification and chirp-assisted sum-frequency generation [20]. The less intense part of the beam (1 μ J, 790 nm) was used to probe the sample excited by the pump pulses. After an appropriate delay and the required shaping of their spectral bandwidth, the probe pulses were sent to the sample ("photonic switch", Fig. 1(b)). The outcoupled spectrum and intensity were monitored by a spectrograph (OceanOptics, HR4000) and a fast photodiode. The traces were recorded by a multichannel analyzer (LeCroy WaveRunner 6100A).

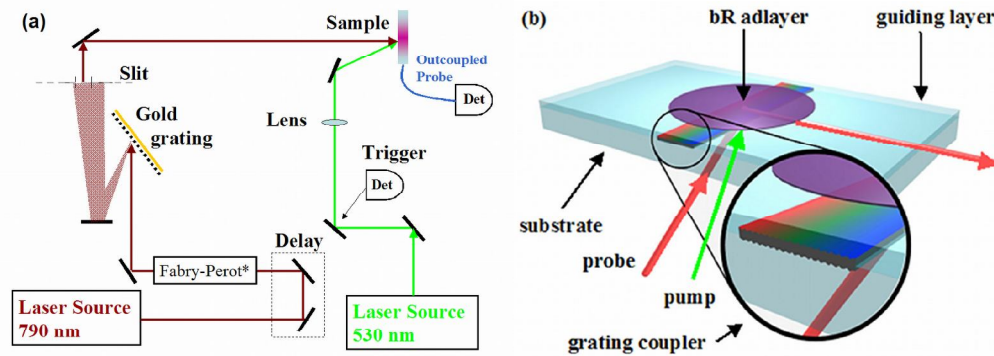


Fig. 1. Experimental setup. (a) The switch was excited by 530 nm pump pulses, and the effects were monitored by probe pulses centered at 790 nm. The traces were detected by a spectrophotometer or a photodiode, and recorded by a multichannel analyzer. The Fabry-Perot interferometer was used only in the sub-picosecond measurements. (b) Scheme of the switch with the incoming/outgoing pulses. A bR adlayer (purple) was deposited above a 1D photonic crystal (coupler grating, rainbow) onto a thin-film optical waveguide (blue) carried by a glass substrate (gray). Probe light: red, pump light: green.

In the first series of experiments the generated pump pulses were left stretched to 45 ps. The probe pulses were sent to a 1800 mm^{-1} gold diffraction grating and the bandwidth was varied by an optical slit between 0.8 nm and 3 nm, providing a pulse duration between 3.2 ps and 12 ps (Fig. 1(a), without Fabry-Perot). Note that these pulses were not transform-limited, as their duration was lengthened by spatial and temporal chirp introduced by the grating.

In the second series (sub-picosecond experiments) the pump pulse was compressed to 150 fs by a transmission grating compressor. The bandwidth of the probe pulse was further narrowed by a Fabry-Perot interferometer (FPI) (finesse ≈ 50) before the gold grating (Fig. 1(a)), so that the grating separated the adjacent orders of the FPI. The resulting temporal and spectral widths of the transform-limited probe pulse were 3 ps and 0.3 nm, respectively. In each case the duration of the pump and probe pulses were carefully measured with an autocorrelator and a cross correlator, respectively, at the sample position.

The photonic switch was fabricated around a slab optical waveguide (Oerlikon Balzers) consisting a glass substrate ($n_s \approx 1.51$) and a thin ($d \approx 200 \text{ nm}$) guiding layer (film) made of high refractive index dielectric material (TiO_2 , $n_F \approx 1.72$). A 1D photonic crystal acting as diffraction grating (2400 lines/mm) was embedded in the waveguide at the substrate-film interface. Under proper conditions the first-order diffracted probe beam was coupled into the guiding layer: The waveguide operates in single mode for wavelengths in the visible range, that is only one transverse electric (TE) and one transverse magnetic (TM) polarized guided

modes exist [21,22]. Besides the wavelength of the measuring light, the propagation constants of these single modes are fully determined by the thickness and refractive index of the film and the refractive indices of the materials surrounding the guiding layer (substrate and bR adlayer). The TE and TM modes can be induced by a resonance incoupling of the measuring light at well-defined angles of incidence [15,21]. The angle of incidence was considered to be positive when turning the sample from its initial position (i.e., when the sample plane was perpendicular to the incident light, Fig. 1(a)) counterclockwise around its symmetry axis defined by the central line of the grating (Fig. 1(b)). During the measurements part of the guiding layer above the grating was covered with a dry patch of bR [15]. The waveguide was placed on a rotational table by which we were able to control the incidence angle of the probe with high resolution ($\approx 10^{-3}$ deg). Once the angle of incidence was fixed to a proper value, so that one of the guided modes (TE or TM, depending on the polarization of the probe beam) could propagate in the layer, the conditions of coupling could be altered by varying the refractive index of the bR layer, that functioned this way as a nonlinear optical (NLO) element of the optical switch.

3. Measurements

For practical reasons, in all of the measurements, the TM resonance peak was used to demonstrate optical switching, corresponding to an angle of incidence of ca. -19.65° . Due to the change of the refractive index of bR following excitation, the coupling wavelength is expected to be shifted by 0.5-1nm at this angle in case of a broadband light (“frequency switch”), or, alternatively, should result in an intensity change in case of a narrow-band light (“amplitude switch”). The effects can be detected by a spectrophotometer or by a photodiode, respectively.

3.1 The ps frequency switch by $BR \rightarrow K$

The first series of measurements aimed to demonstrate the $BR \rightarrow K$ switch in the picosecond range. In order to detect the wavelength shift of the coupled light due to fast excitation of bR, the full-width-at-half-maximum bandwidth (FWHM) of the linearly polarized probe pulses of 12 ps was chosen to be 3 nm. The spectrum selected by the waveguide was then measured by a spectrophotometer. The bR photocycle was initiated by a pump pulse with duration of 45 ps, hitting the sample 100 ps before the probe pulse. Under these conditions, the only intermediate present in the photocycle is the K form, with a red-shifted absorption spectrum relative to the ground state (BR). Such a spectral shift should result in a refractive index increase in the adlayer at wavelengths longer than that of the absorption peak [14]. This, in turn, should change the coupling conditions such that the wavelength of the incoupled light, selected by the grating coupler, is shifted to the red, provided that the angle of incidence is unchanged (Fig. 2(a)). In fact, the traces in Fig. 2(b) show a red-shift in the spectrum of the incoupled light upon excitation. Such type of switching we call “frequency switching”, because using this effect one can select different frequency bands of very narrow bandwidth ($\Delta\lambda < 1\text{nm}$ in our case) of a broadband pulse, enabling frequency demultiplexing, an essential operation in optical information processing (see also Conclusion).

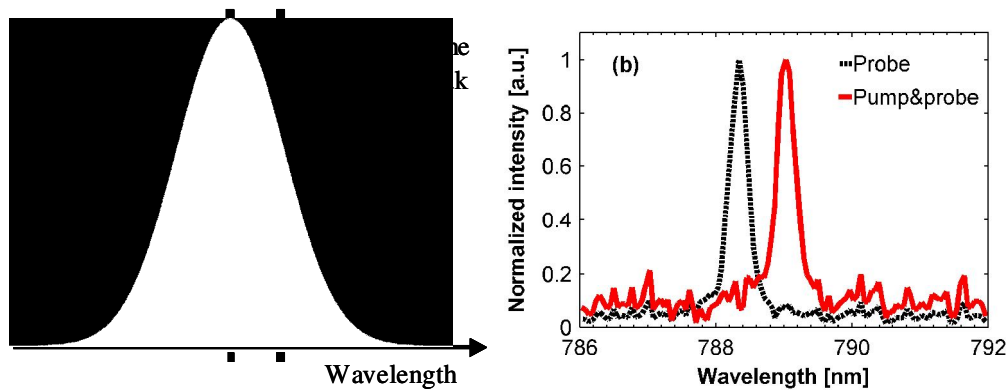


Fig. 2. Spectral shift of the incoupled light, initiated by the pump pulse. (a) Schematic representation of the spectral change: Excitation of the sample induces a refractive index increase of the bR adlayer, resulting in a red-shift of the resonance peak of the grating coupler (dashed line) at a fixed angle of incidence. As a consequence, a red-shifted narrow band is selected from the broad spectrum (indicated by the red-orange Gaussian). (b) The measured spectrum of the incoupled light at a fixed angle before (probe) and after (pump & probe) the excitation of the sample.

According to our calculations based on the wave equations of grating-coupled single-mode waveguides [15,21,22], the amount of the shift is consistent with a refractive index change of ca. 3×10^{-3} of the bR adlayer, comparable to that observed between BR and M, and allowing a direct “amplitude switching” [14–16].

3.2 The ps amplitude switch by $BR \rightarrow K$

In order to realize amplitude switching by the K intermediate, next the bandwidth of the probe pulses was narrowed down to 0.8 nm. The intensity of the coupled light was monitored by a low noise (nanosecond) photodiode. (Note that the actual time resolution of the switch is determined not by the photodiode, but by the time delay and duration of the pump and probe pulses.) In order to maximize the effect, the angle of the incident pulse was slightly tuned by turning the sample counterclockwise (CCW), off the resonance peak, until the output intensity reached the half-maximum [15]. When the switch is turned on by the green pump pulse, under such conditions the refractive index change is expected to shift the resonance peak so that the intensity of the incoupled light increases (Fig. 3(a)). From the measured intensities of the incoupled pulses one can see that when both the exciting and measuring lights hit the sample, the incoupled intensity (Meas. p&p, Fig. 3(b)) is considerably larger than the incoupled light when only the probe beam is present (Probe). Note that a small amount of stray light also reached the detector when the exciting pulse was on (Pump). Correcting to this (Corr. p&p), the fast intensity modulation achieved in this pilot experiment was in the range of 50%.

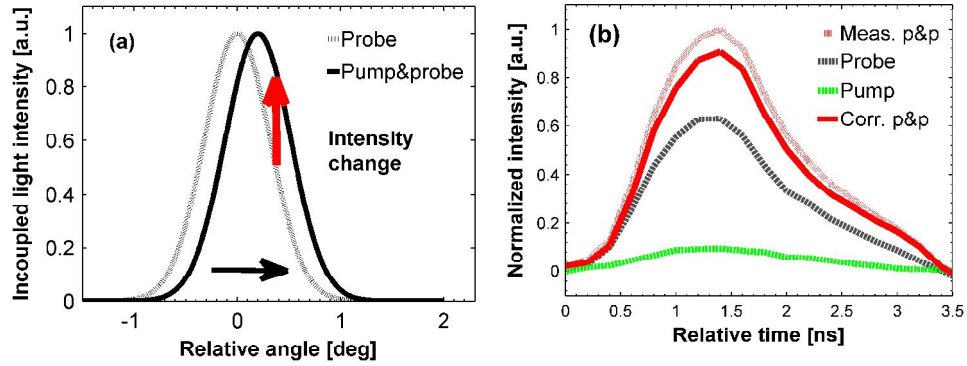


Fig. 3. (a) Demonstration of the shift of the resonance peak of the incoupled light intensity in a thin-waveguide grating coupler device upon a hypothetical refractive index increase of the adlayer. The red arrow indicates the expected intensity change at the counterclockwise half maximum of the original resonance peak. (b) Outcoupled light intensity when the pump and probe pulses came together (with 100 ps probe delay, dotted red line, Meas. p&p), or separately (gray dashed: probe only, green dashed: scattered-in pump only), as detected by the photodiode. The solid red curve shows the real p&p signal corrected by the scattered-in pump pulse (i.e., the algebraic difference of the dotted red and green traces). Note that the time course of the signal represents the response of the photodiode only, not that of the actual light pulse.

3.3 The femtosecond amplitude switch by $BR \rightarrow I$

To explore the possibility of the photonics application of the fastest spectral transition of the bR photocycle ($BR \rightarrow I$), in the next experimental series the duration of the pump and the probe pulses were considerably shortened to 150 fs and 3 ps, respectively. Figure 4(b) shows the relative intensities of the output probe pulses detected at the half-maximum on CCW side of the resonance peak, both without excitation of the bR adlayer and with a pump pulse arriving at zero time delay to the sample (i.e., the intensity maxima of the pump and probe pulses coincided in time, see also Fig. 5).

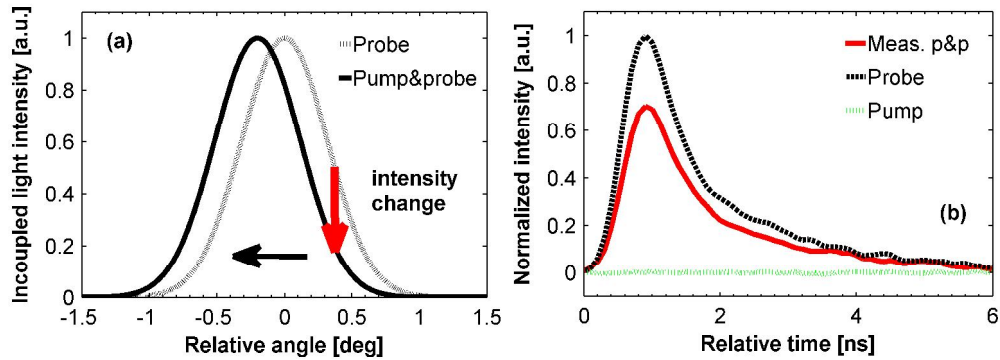


Fig. 4. Ultrafast experiments. (a) Demonstration of the shift of the resonance peak of the incoupled light intensity in a thin-waveguide grating coupler device upon a hypothetical refractive index decrease of the adlayer. The red arrow indicates the expected intensity change at the counterclockwise half maximum of the original resonance peak. (b) Intensities of the probe pulses incoupled at the half-maximum on the long-wavelength side of the resonance peak, measured without (dashed) and with excitation at zero delay (solid).

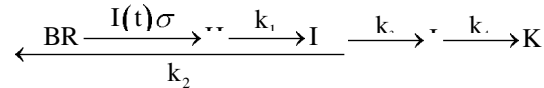
As one can see, now the intensity of the coupled pulse without excitation is higher than that when the pump pulse initiated the photocycle. This can be interpreted as a shift of the coupling peak in the direction opposite to that for the K intermediate described above, meaning that the refractive index of the adlayer decreases upon excitation (Fig. 4(a)). Such an

effect is consistent with the assumption that in this case amplitude switching is dominated by the I intermediate of the bR photocycle, since the main absorption peak of I is considerably blue-shifted ($\lambda_{\text{max}} = 460\text{nm}$) relative to that of BR ($\lambda_{\text{max}} = 570\text{nm}$).

4. Discussion

To check this hypothesis, we performed a kinetic analysis of the fast reactions of the bR photocycle. At very short times for the duration of the applied pump and probe pulses, a mixture of the I, J and K intermediates will coexist during the pump pulse (that was chosen to have a duration of 3 ps to yield narrow spectral bandwidth). Using the published rate constant values of these intermediates [12,23–25], their relative contribution to the light-induced change of the probe signal was determined [Fig. 4(b)]. In order to estimate these contributions to the optical signals detected by our ultrafast measurements, we simulated the development (and decay) of H, I, J and K during the time course of the probe pulse, based on the experimental conditions and the data available in the literature. Several experimental and theoretical studies have been performed to reveal the fast intramolecular events after photoexcitation of bacteriorhodopsin (bR) [12,26–29]. According to a consensus view, a quasistationary electronic excited state (I_{460}) of bR is formed from the Franck-Condon excited state (H_{560}), and followed by an electronic transition to J_{625} . A subsequent vibrational relaxation process leads to the K_{610} -state containing a 13-cis isomerized retinal chromophore.

In our ultrafast experiments, the photocycle was initiated by an intense (3 mJ/cm^2) and short ($\tau = 150 \text{ fs}$) pump pulse. The 3 ps probe pulse was used to monitor the refractive index change of the dried bR sample after the excitation. On the time scale of the probe pulse, all the early intermediates were concurrently present in the sample, hence the recorded signal contained contributions from all these intermediate states. The following photocycle scheme (including the ground state: BR) was used in the calculations:



The absorption cross section of BR (σ) at 530nm is $0.76 \cdot 10^{-16} \text{cm}^2$. The first-order rate constants of the transitions are indicated above the corresponding arrows. The exciting $I_{\text{pump}}(t)$ pulse was modeled with an FWHM-value of $\tau = 150 \text{ fs}$. The concentrations of the intermediate states were calculated by numerically solving the following first-order rate-equation system:

$$\begin{aligned} \frac{d}{dt}[BR] &= -I_{\text{pump}}(t)\sigma[BR] + k_3[I] \\ \frac{d}{dt}[H] &= I_{\text{pump}}(t)\sigma[BR] - k_1[H] \\ \frac{d}{dt}[I] &= k_1[H] - (k_2 + k_3)[I] \\ \frac{d}{dt}[J] &= k_2[I] - k_4[J] \\ \frac{d}{dt}[K] &= k_4[J] - k_3[K] \end{aligned}$$

Here $[X](t)$ denotes the time-dependent concentration of the X intermediate (including the ground state (BR)) and k_i is the first-order rate constant corresponding to the i^{th} transition.

The following rate constants were used in the computations performed under MATLAB using the Newton method:

- $1/k_1$ is the rise of the I-state (30 fs) [26,29],
- k_2 and k_3 were determined from the decay of the I-state: $1/(k_2 + k_3) = 500$ fs [27,28], moreover, k_3/k_2 is calculated from the experimentally determined “quantum efficiency” of the photocycle (i.e., the probability by which an excited-state molecule proceeds to J and further on). In dry samples this was found to be 63% [12], hence $k_3/k_2 = 63/37$.
- k_4 was defined by the time constant of the accumulation of the K intermediate (3 ps).

The unweighted contribution of each intermediate state to the signal can be determined by integrating the convolution of measuring $I_{\text{probe}}(t)$ pulse (FWHM = 3ps) and the corresponding concentrations ($[X(t)]$). Note that due to the negligible spectral shift between BR and H, major spectral changes start only by the development of the I intermediate. Hence, the contribution of H to the measured effect can be neglected, and for the sake of simplicity, it is omitted from Fig. 5.

The final values of the integrals gave the non-weighted contributions of each state (after H) to the measured signal: 53%, 39% and 8% for the I, J and K-states, respectively. To get the actual contributions, these values should be weighted by the difference refractive index spectra of the intermediates relative to BR at 788 nm [14]. Taking into account that the larger spectral shift between BR₅₇₀ and I₄₆₀ should correspond to a higher absolute refractive index change than the J₆₂₅-BR₅₇₀ and K₆₁₀-BR₅₇₀ differences, the above results indicate a clear dominance of the BR-I transition in the measured signal.

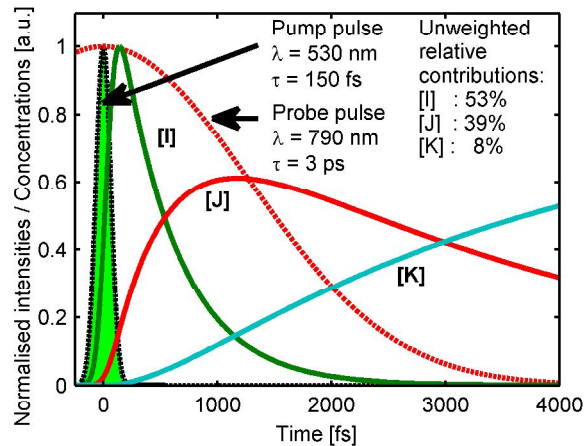


Fig. 5. Simulation of the time course of the pump and probe pulses and the concentrations of the I, J and K intermediates. The calculated unweighted contributions of the intermediates to the measured signal are listed.

Hence we can conclude here that the effect is dominated by the I intermediate (ca. 53%), while the subsequent J and K intermediates have a considerably smaller effect on the short probe pulse (ca. 39% and 8%, respectively). The magnitude and direction of the spectral shifts of the main absorption peaks of I, J and K relative to BR (110nm blue, 55nm red and 40nm red, respectively) should further enhance the blue-shift character of the effect detected at zero time delay, in agreement with the experiment.

5. Conclusions and outlook

The above results clearly demonstrate the feasibility of ultrafast all-optical frequency and amplitude switching using two photoreactions (the picosecond BR→K and the subpicosecond BR→I transitions) of the bR photocycle. More effective switching is expected to be achieved

in the future by proper modification of the protein sample (e.g. the photocycle can be stopped at the I or K intermediates by chemical modification of the chromophore) or cooling, respectively [26,30], and optimizing the underlying photonic structure. The demonstrated principles may be utilized in future protein-based integrated optical devices. Frequency switching, e.g., can serve as a basis of frequency demultiplexing, a crucial operation of high-bandwidth optical information technology, where a broadband pulse can be separated to several narrow-frequency bands, allowing their independent coding or decoding by amplitude switching. With the use of such devices, all-optical switching technology can be revolutionized, pushing the present state of the art of a few times 10 GHz well beyond the THz barrier.

Acknowledgments

This work was supported by the Hungarian research grants OTKA CK-78367, K-75149 and by NATO SFP 974262. The authors are indebted to Dr. Francesco Vita for helpful suggestions concerning the experiments, and to Mr. András Makai for his technical assistance.